A New Approach to the High Resolution Electrodeposition of Metals via the Feedback Mode of the Scanning Electrochemical Microscope

Daniel Mandler* and Allen J. Bard*

Department of Chemistry, The University of Texas at Austin, Austin, Texas 78712

ABSTRACT

Gold and palladium electrodeposition in polymer films immersed in solution with high resolution has been accomplished using the scanning electrochemical microscope (SECM). The SECM was used in the feedback mode, where hexaamminoruthenium(III), $Ru(NH_3)_6^{3+}$, was reduced at an ultramicroelectrode (UME) and diffused to a protonated polyvinyl pyridine-coated surface. When metal anions, *e.g.*, $AuCl_4^-$ or $PdCl_4^{2-}$, were incorporated in the polymeric matrix, the diffusion of reduced mediator, $Ru(NH_3)^{2+}$, from the UME to the polymer film resulted in metal deposition. The different factors that determine the size and pattern of deposited metal were examined. The difference between gold and palladium deposition was studied by several techniques and interpreted in terms of kinetic and thermodynamic properties of the mediator and the metal complex.

We introduce here a new method for depositing metals with high resolution with the scanning electrochemical microscope (SECM) by using a redox mediator and describe experiments on the deposition of Pd and Au in a polymer matrix. The desire for smaller and smaller devices, especially in microelectronics, has resulted in the development of new techniques (1) such as x-ray lithography for high resolution pattern production. These techniques are applied in integrated circuit production, where patterns of the order of several tenths of a micron are formed. Intensive efforts are still being made (2) to find new techniques with higher resolution and to fabricate masks for x-ray and UV lithography.

One approach to high resolution fabrication has involved the use of the scanning tunneling microscope (STM) (3). An alternative technique involves the use of the SECM. Several studies from our laboratory (4-6) have demonstrated the application of the SECM to characterize surfaces immersed in an electrolyte and to etch and deposit features. With the SECM an ultramicroelectrode (UME) tip whose motion is controlled by piezoelectric elements (as in the STM) is scanned over the substrate surface. The faradaic current that flows between the UME and the substrate promotes the desired reactions at the tip and at the surface. Metal deposition and etching have been achieved (6) by scanning a small tip over a substrate coated with an ionically conductive polymer that contains metal ions. The application of a negative potential to the tip causes the direct reduction of metal ion in the polymer at the tip and etching of the metal substrate below the polymer film. Alternatively, a negative potential applied to the substrate leads to metal deposition on the substrate and an oxidation process at the tip. Submicron patterns have been produced at the tip by this approach. In this direct deposition and etching approach, the polymer film is exposed to air and plays the role of the electrolyte. The size of the pattern produced is largely a function of the electrical field (and current density) distribution.

The characterization of surfaces of different substrates (both conductors and insulators) has also been carried out with the SECM in solutions containing a redox active species (4, 5). In one approach (called the feedback mode) the distance between the UME and the surface is monitored and determined by changes in the faradaic current. An increase in the current (positive feedback current) is caused by the regeneration of the redox species electrolyzed at the UME when the electrode approaches a conductive surface. A decrease in the current, due to the hindrance of the hemispherical diffusion to the UME, occurs when the electrode approaches an insulator. Conductive and insulating surfaces have been mapped in this way to provide topographic surface scans (5).

However, no attempts have previously been made to use the feedback mode for the high resolution modification of surfaces immersed in solutions. Because an electron transfer process occurs between the generated redox couple and the surface, this approach can clearly be used to drive electrochemical reactions on surfaces (Fig. 1). The feedback mode of surface modification is different than the direct mode in that the deposition reaction occurs through reaction of a soluble tip-generated species with a suitable metal precursor in the polymer film, rather than directly at the tip. In the feedback deposition mode, the polymer film is immersed in a solution containing electrolyte and a redox species. Here we report the successful electrodeposition of gold and palladium using this approach. A reduced mediator is used both as a means to control the distance between the UME and a surface, and in addition, to reduce metal ions which are incorporated in a polymeric film.

Experimental

The SECM was based mainly (6) on a micropositioning device (Burleigh Instruments, Burleigh Park, Fishers, New York) that controlled the movements of three piezoelectric drivers (inchworms). The speed of these drivers could be varied from 100 Å/s to 2 mm/s. The sample was attached to the x-y stage, while the UME was mounted on the z piezoelectric drive. The SECM was mounted on an NRC pneumatic isolation mount (Newport Corporation, Fountain Valley, California) and shielded with a copper screen Faraday cage.

The ultramicroelectrode (UME) was biased with a Princeton Applied Research (PAR, Princeton, New Jersey) Model 173 potentiostat, and the current, as a function of time or voltage, was recorded on a chart recorder. Cyclic voltammetry was carried out with either the PAR potentiostat or a BAS 100 electrochemical analyzer. UV-visible

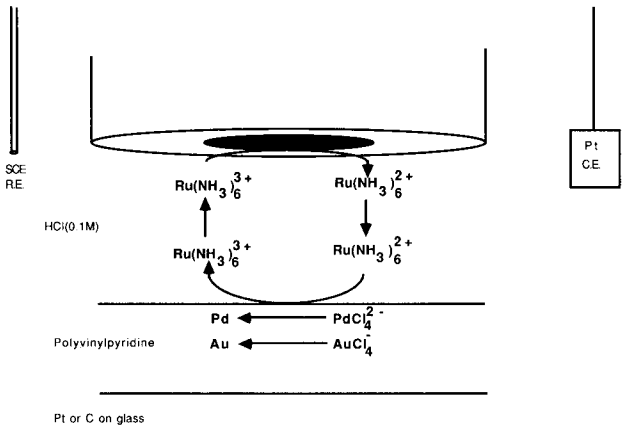

Fig. 1. Overall scheme for the deposition of gold and palladium using the SECM in the feedback mode.

* Electrochemical Society Active Member.

spectra were measured by an HP8450A spectrophotomer (Hewlett Packard, Palo Alto, California). The thickness of the polymer films was detemined by an Alpha-step 200 profilometer (Tencor Instruments, Mountain View, California) and the electron micrographs were taken with a scanning electron microscope (SEM, Jeol JSM-35C) equipped with an electron dispersive spectrometer (EDS, Kevex Analyst 8000, Kevex Corporation, Foster City, California) for elemental analysis.

Palladium chloride, $PdCl_2$, and hexaammine ruthenium(II) dichloride, $Ru(NH_3)_6Cl_2$, were purchased from Alfa Products (Danvers, Massachusetts). Polyvinylpyridine (PVP, M.W. *ca.* 200,000) was ordered from Scientific Polymer Products, Incorporated, (Ontario, New York). Propyl viologen sulfonate (PVS) was synthesized according to a literature procedure (7). All other chemicals were purchased from Aldrich (Milwaukee, Wisconsin). Milli-Q reagent water (Millipore) was used for the aqueous solutions. Platinum (10-50 μm diam) and carbon (11 μm) UME sealed in a glass capillary were fabricated as described previously (4). A glassy carbon disk electrode (BAS 3.0 mm diam) was used for cyclic voltammetry experiments. Quartz disks 0.5 in. diam (ESCO Products, Oak Ridge, New Jersey) were used as substrates.

The spin coating solution contained 0.67% weight percent (w/o) PVP and 0.067% (w/o) 1,6-dibromohexane as a cross-linking agent dissolved in 2-propanol. Platinum-sputtered quartz disks, carbon-deposited quartz disks, and indium tin oxide (ITO) rectangles were spin coated with five drops of the 2-propanol solution at 5000 rps and left at 90°C for at least 18h.

In a typical experiment a PVP spin-coated substrate was attached to a small, flat Teflon cell and soaked in a 0.1*M* HCl solution containing 0.05*M* metal complex, *e.g.*, $NaAuCl_4$, for 30 min. The sample was then carefully washed with water and placed in the SECM. The UME was brought close to the surface (*ca.* 1 mm) and a 10 m*M* solution of the mediator in 0.1*M* HCl was added. A saturated calomel reference electrode (SCE) was immersed into the Teflon cell, which also contained a platinum wire counter-electrode. The sample was left to equilibrate for 15 min before the UME was made to approach the surface. The current as a function of time was recorded upon approaching the surface and translated later into a current-distance curve using the SECM calibration curves for insulating substrates (5) and the approach speed. When several experiments were carried out with the same sample, the potential was turned off and the UME was backed slightly away from the surface before moving it to another spot. The UME could be brought to the same distance from the surface by moving it towards the surface until exactly the same current was measured.

For cyclic voltammetry experiments, the glassy carbon electrode (GCE) was spin coated with five drops of the PVP solution (5000 rps). The background was first measured after allowing the electrode to equilibrate for 10 min in 0.1*M* HCl solution. Then the electrode was soaked in the metal complex solution for 30 min and rinsed with water; the voltammogram was recorded 5 min after the electrode was immersed in 0.1*M* HCl.

UV-visible spectra were recorded after the PVP/ITO samples were soaked in the metal complex solutions for 30 min and rinsed with water.

Results

Deposition of Au and Pd by generation of $Ru(NH_3)_6^{2+}$.—When a sufficiently negative potential (−0.3V *vs.* SCE) was applied to a UME, which was held far from any surface, and immersed in a solution containing 10 m*M* $Ru(NH_3)_6^{3+}$ and 0.1*M* HCl, $Ru(NH_3)_6^{2+}$ was formed and a steady-state current was reached within a few seconds. The steady-state current was smaller, when the UME was held near (several microns) a PVP-coated surface. This negative feedback current was not dependent on the type of substrate used below the insulating PVP film; *i.e.*, platinum, carbon on glass, or glass. Moreover, similar current *vs.* UME-surface distance curves were obtained with polymers of different charge, such as protonated PVP (positively charged) and Nafion (negatively charged). However, when the PVP-coated substrates contained $AuCl_4^-$, very different behavior was found. As the electrode approached the surface, the current first increased above the steady-state value (signaling positive feedback or regeneration of $Ru(NH_3)_6^{3+}$ at the PVP surface) followed by a rapid decrease (as the reactant causing regeneration was depleted). SEM pictures (Fig. 3a) show that while gold disks are formed, the gold distribution inside the disk is not uniform. The inner part of the disks contains small gold particles, as confirmed by EDS, while the outer part is darker and contains fewer gold particles. Sometimes the outer parts of the disks could be washed away with water. A gold complex is probably first produced, and upon continuous electrolysis, it is further reduced to gold. The initial electron transfer process between $Ru(NH_3)_6^{2+}$ and $AuCl_4^-$ is very fast, as shown by the effect of increasing the speed of approach of the UME to the surface (Fig. 2a). The increase of the positive feedback current means that the reduced mediator is oxidized by the surface fast enough to respond to sudden changes in the concentration of $Ru(NH_3)_6^{2+}$ on the surface. This fact allowed the production of patterns other than disks, as shown in Fig. 3b. For example, when the UME is scanned over the surface at a constant distance, which is maintained by holding the current constant, the gold complex is reduced, and as a result, a line is formed. The width of the line is governed by the speed of the scan as shown in Fig. 3b, as well as by other parameters, which are discussed later. Note that the line is mainly composed of a gold complex and is not a metallic gold line as is proved by EDS and SEM (compare Fig. 3a and b).

On the other hand, when the PVP-coated substrate was first soaked in $PdCl_2$/HCl, only a current decrease was observed when an UME was moved towards it under similar solution conditions, and palladium rings were formed (Fig. 3c). Increasing the speed of UME approach to 23 μm/s did not result in a positive feedback current. To form the

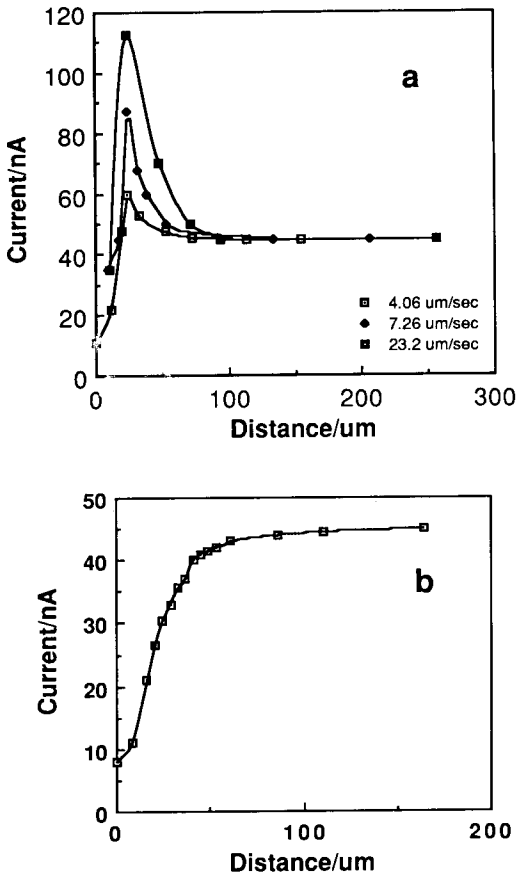

Fig. 2. Steady-state current of a 25 μm Pt UME (E = −0.3V *vs.* SCE) as a function of distance from a PVP-coated substrate in a 10 mM $Ru(NH_3)_6^{3+}$/0.1M HCl solution. (a) After soaking the substrate in 0.05M $NaAuCl_4$/0.1M HCl solution, (b) after soaking the substrate in 0.05M $PdCl_2$/0.1M HCl solution.

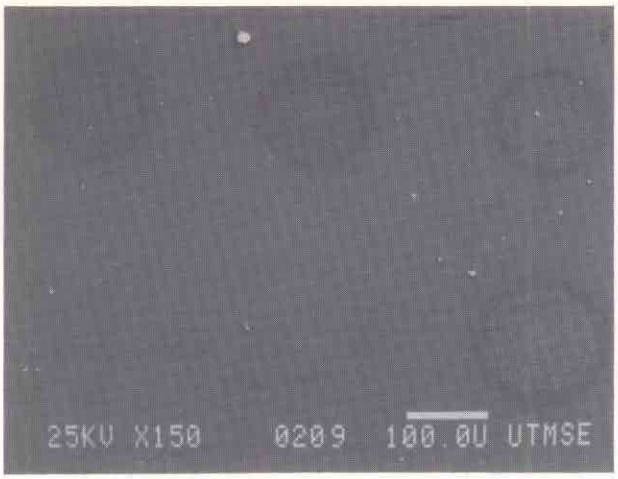

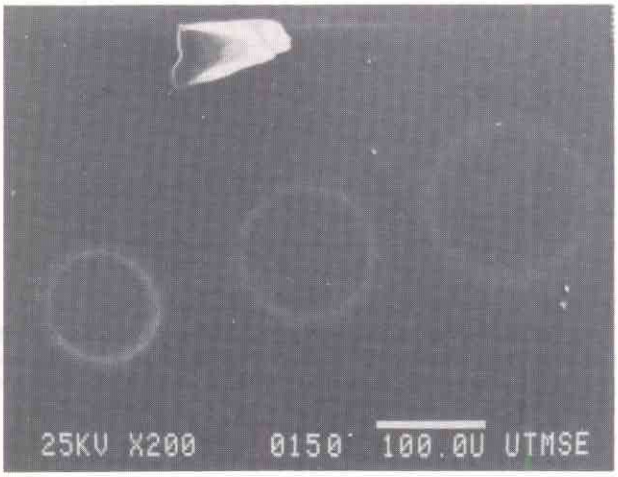

Fig. 3. Scanning electron micrographs: (a, top left) gold disks formed upon leaving a 10 μm Pt UME ($E = -0.3$V *vs.* SCE) at various distances from a $AuCl_4^-$/PVP-coated substrate for 5 min per pattern. (b, above) A line formed by scanning with a 10 μm Pt UME ($E = -0.3$V *vs.* SCE) over a $AuCl_4^-$/PVP-coated substrate at two different speeds (2.3 and 1.27 μm/s). (c, left) Palladium rings produced with a 25 μm Pt UME that was held at −0.3V *vs.* SCE for 30 min per pattern over a $PdCl_4^{2-}$/PVP-coated surface.

Pd rings, the biased UME had to be left for a longer time (at least 8 min) above the polymer film compared to the gold samples. Control experiments did not reveal any kind of patterns on the polymer when the PVP had not been presoaked in a metal ion solution.

Factors determining size and shape of patterns.— Various experiments were conducted to examine the factors that affect the size and shape of the patterns. We found at least four extrinsic parameters that determined the structure of the metal deposit. The size of the pattern was linearly dependent on the distance between the UME and the surface, as can be seen in Fig. 4. This was true for both the gold disks and the palladium rings. Furthermore, the size of the structure formed depended on the ratio of the radius of the insulator in which the Pt or C was embedded and the radius of the Pt or C. The smaller the insulator, the bigger were the disks or rings that were produced (Fig. 4a). The size of the Pt or C electrode itself (usually 25 μm) affected the steady-state current as well as the size of the pattern. Smaller electrodes, down to 10 μm diam, yielded smaller gold disks (Fig. 4b).

An important factor in the size of the deposited feature was the time that the biased UME was held close to the surface. In the case of gold, the radii of the disks formed depended on the square root of time, as shown in Fig. 5b. However, this dependence was observed only for disks that were smaller than the insulator size. As shown in Fig. 5a, the rate of growth of the gold disks was much slower once the radius reached that of the UME (*ca.* 120 μm). Note that when $PdCl_2$ was used, the rings did not grow in radius as a function of time, but became clearer, *i.e.*, more palladium was deposited in the same region.

Clearly, the most striking difference in the shape of the deposits are produced when the metal complex is varied. As mentioned before, gold disks were formed when PVP was soaked in a solution of $NaAuCl_4$/HCl, while palladium rings were detected when the same polymer was soaked in a $PdCl_2$/HCl solution. To account for this behavior, several different types of experiments were carried out.

Spectroscopic measurements were made to determine metal ion concentrations in PVP films coated on indium tin oxide (ITO) electrodes. Figure 6 shows the spectra of PVP/ITO electrodes which were soaked in HCl/$AuCl_4$ and HCl/$PdCl_2$ solutions, before and after applying a negative potential to the ITO electrodes (−0.35V *vs.* SCE). As can be seen, not only was the concentration of $AuCl_4^-$ ($\epsilon_{313} = 5.4 \times 10^3\ M^{-1}\ cm^{-1}$) higher than that of $PdCl_4^{2-}$ ($\epsilon_{279} = 6.5 \times 10^3\ M^{-1}\ cm^{-1}$) in the PVP/ITO, but upon applying a negative potential, only minor changes could be detected in $PdCl_4^{2-}$ spectrum, while the $AuCl_4^-$ absorbance completely disappeared.

Cyclic voltammetry experiments were undertaken to gauge the ease of penetration of the $Ru(NH_3)_6^{2+}$ into the PVP films and to examine the reduction waves of the metal complexes contained in the films. Figure 7 shows different cyclic voltammetry experiments. To determine whether the reduced mediator, $Ru(NH_3)_6^{2+}$, penetrated the positively-charged PVP, the cyclic voltammetry of the mediator was examined at a bare electrode and the behavior compared to that at a PVP-coated electrode (Fig. 7a). The cathodic current at the coated electrode was 86% of the bare electrode value, indicating that the reduced species, $Ru(NH_3)_6^{2+}$, easily penetrated the polymer. Significant differences were observed between the cyclic voltammetry of a PVP-coated electrode that was immersed in a $NaAuCl_4$/HCl *vs.* a $PdCl_2$/HCl solution (Fig. 7b, c). Neither voltammogram is reversible, and both show a reduction wave on the first scan, presumably due to the reduction of $AuCl_4^-$ and $PdCl_4^{2-}$ to gold and palladium, respectively. The reduction of the gold complex occurs at 0.46V *vs.* SCE with a cathodic peak current, i_{pc}, of 39.2 μA, while the reduction of the Pd complex occurs at −0.32V *vs.* SCE with an i_{pc} of 15 μA. These results can be compared to the cyclic

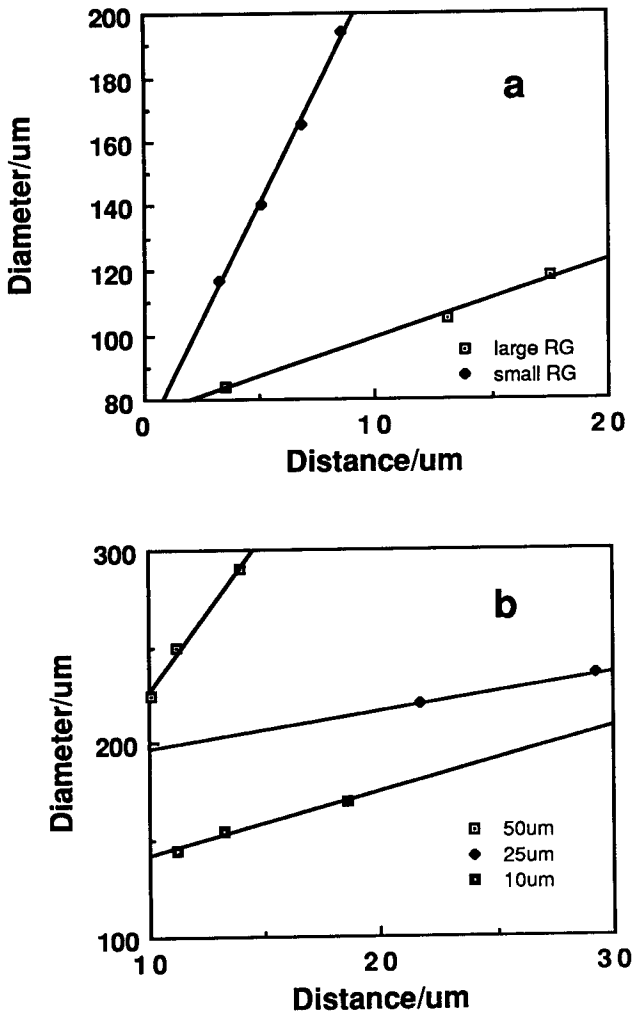

Fig. 4. The dependence of the diameter of gold patterns as a function of distance between the UME and the surface. (a) 25 μm Pt UME and different insulator-to-electrode radii ratios (*RG*): *RG* large *ca.* 10; *RG* small *ca.* 6. (b) With different Pt electrodes and a large insulator-to-electrode radius ratio (*RG* > 10).

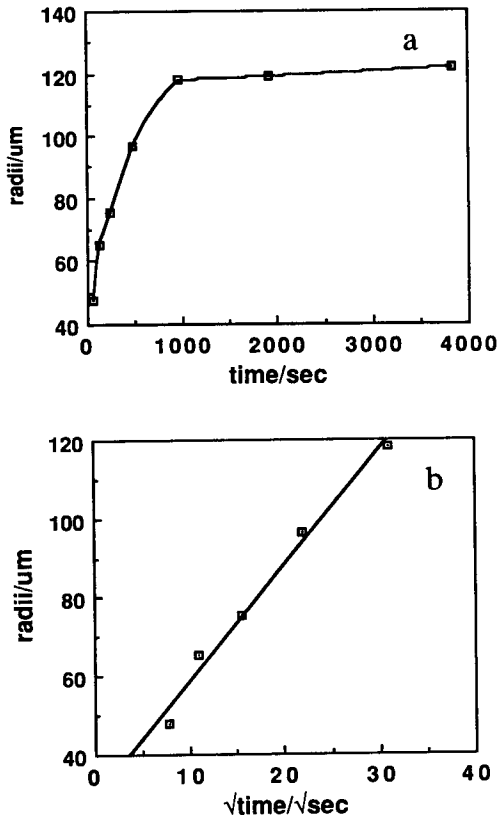

Fig. 5. The dependence of the radii of gold patterns as a function of electrolysis time (a) and as a function of the square root of time for patterns smaller than the insulator diameter (b).

voltammetry of these complexes in homogeneous solution. The cathodic wave of $AuCl_4^-$ in the film occurred at more positive potentials (by 90 mV), while the cathodic wave of $PdCl_4^{2-}$ in the film occurred at more negative potentials (by 160 mV) (Fig. 7b, c).

Several experiments were carried out with more negative redox couples as mediators in place of $Ru(NH_3)_6^{3+}$. Methyl viologen, MV^{2+}, and propyl viologen sulfonate, PVS, are reduced at −0.75V *vs.* SCE at a carbon UME (11 μm). A carbon electrode was used here to prevent hydrogen evolution in this acidic medium (0.1*M* HCl). Both gold and palladium formed disks, when the viologens were used as mediators.

Mixing solutions of $PdCl_4^{2-}$ with $Ru(NH_3)_6^{2+}$ with rapid magnetic stirring gave an essentially instantaneous color change, with a precipitate forming at concentrations above 0.02*M*. These results suggest that the homogeneous reaction is very rapid. A remarkable change in the SECM current-distance response with Pd(II) was noticed when Cl^- was replaced by Br^-, [*i.e.*, when $Pd(NO_3)_2$ in HBr was used rather than $PdCl_2$ in the film]. A slightly positive feedback current was observed and Pd disks were formed (Fig. 8). Figure 6 shows the UV/visible spectra of a PVP/ITO electrode soaked in a solution of $Pd(NO_3)_2$ in HBr before and after applying −0.35V *vs.* SCE. The cyclic voltammogram of a glassy carbon electrode coated with PVP and soaked with the same solution is shown in Fig. 7d. The cyclic voltammogram reveals a cathodic wave with i_{pc} of 58 μA at −0.24V *vs.* SCE, which is only slightly shifted (*ca.* 10 mV) compared to that in homogeneous solution.

Discussion

The theory of an UME in homogeneous solution is well established (8). According to this theory, the steady-state current at a disk UME in a solution that contains an electroactive species at concentration C^* is given by Eq. [1]

$$i = 4nFDrC^* \quad [1]$$

where n is the number of electrons transferred, **F** is the Faradaic constant, D is the diffusion coefficient, and r is the UME radius. However, when an UME approaches a surface, this equation no longer holds either because of an electron transfer reaction that occurs on the surface or because of hindrance of the flux of electroactive species to the UME (4, 5). Thus, changes in the steady-state current are observed when the distance between the electrode and the surface is of the order of the UME diameter. In other words, the distance between the UME and the surface can be controlled and determined by measurement of ratio of the steady-state current with respect to the long distance value. This is the basic concept in the use of the SECM for topographic mapping of a surface.

Accordingly, an increase of the steady-state current (positive feedback current) is observed when a biased (−0.35V *vs.* SCE) Pt UME (25 μm diam) approaches a platinum surface in a 10 m*M* $Ru(NH_3)_6^{3+}$/0.1*M* HCl solution. Note that the surface is not connected to an external source, but its potential is poised by the contacting solution, which governs the substrate potential. The positive feedback current is due to the regeneration of the oxidized species, $Ru(NH_3)_6^{3+}$, on the metal surface. The magnitude of the increase in the current fits the theoretical treatment recently proposed (4, 5).

On the other hand, when the surface is spin coated with an ionically conductive polymer, *e.g.*, protonated PVP, a current decrease is found. The thickness of the polymer used was 0.1-0.2 μm. This means that no electron transfer occurred between the reduced mediator and the polymer, which also effectively blocked the underlying Pt from contact with $Ru(NH_3)_6^{2+}$. When Nafion was used as a coating

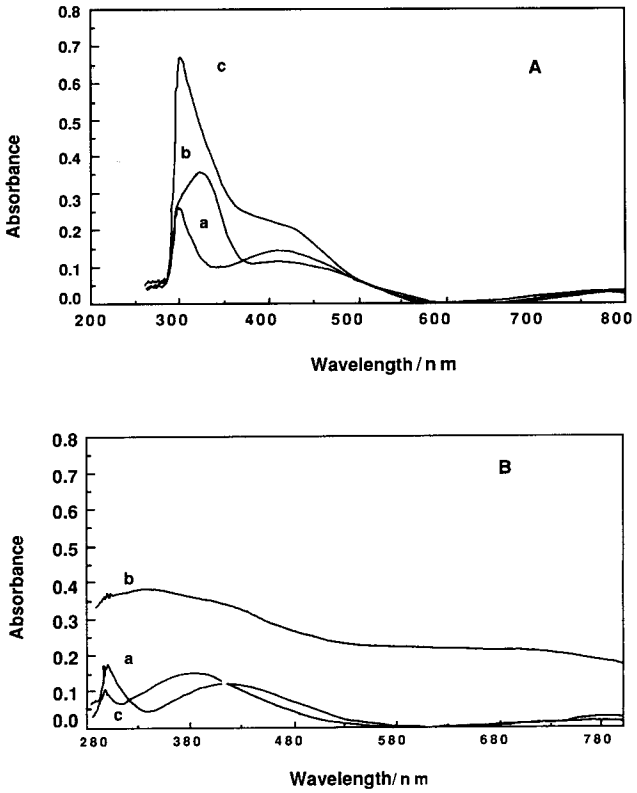

Fig. 6. The UV-visible absorbance spectra of PVP/ITO samples soaked in (a) 0.05M $PdCl_2$/0.1M HCl solution; (b) 0.05M $NaAuCl_4$/0.1M HCl solution; (c) 0.05M $Pd(NO_3)_2$/0.1M HBr solution, before (A) and after (B) applying −0.35V *vs.* SCE.

polymer, the same decrease in current of the UME was observed when the UME approached the film. Since the Nafion film contained $Ru(NH_3)_6^{3+}$, which was exchanged into the film upon contact with the mediator solution, the result suggests that the rate of the electron self-exchange reaction between $(Ru(NH_3)_6^{3+})_{Nafion}$ and $(Ru(NH_3)_6^{2+})_{soln}$ was too slow to cause significant regeneration of the 3+ species in solution.

The film was used to attach electroactive species to the surface. Protonated PVP has been extensively studied (9) as a means of attaching negatively charged species, such as $Mo(CN)_8^{4-}$ and $Fe(CN)_6^{3-}$, to an electrode surface. We have shown here that anions, *e.g.*, $PdCl_4^{2-}$ and $AuCl_4^-$, are also strongly adsorbed on protonated PVP. The UME response found in SECM for an electronically insulating polymer film containing a finite amount of an electroactive species, *e.g.*, $AuCl_4^-$, is different than that found with either an electronically conductive or insulating substrate (Fig. 2a). As the UME approaches the surfaces, a positive feedback current is first detected. However, the current decreases to a level below the steady-state value, even when the electrode is kept at a constant distance. This clearly indicates that the reduced mediator (*i.e.*, $Ru(NH_3)_6^{2+}$) is first oxidized by the gold complex, but the current decreases when the $AuCl_4^-$ contained in the film below the UME has been consumed. Indeed, metallic gold structures are seen in the film when the UME is removed (Fig. 3a). The reduction of $AuCl_4^-$ by $Ru(NH_3)_6^{2+}$ was examined by Lever and Powell (10) and involves a rather complicated reaction sequence. The first process yields a purple complex, which undergoes further reduction to form gold (Eq. [2]). The overall reaction is

$$3Ru(NH_3)_6^{2+} + AuCl_4^- \rightarrow 3Ru(NH_3)_6^{3+} + Au + 4Cl^- \quad [2]$$

A PVP film soaked in a palladium chloride complex solution shows a different behavior. A current decrease is always found (Fig. 2b), indicating that the electron transfer process between $Ru(NH_3)_6^{2+}$ and the metal anion is much slower. A careful examination of the current-distance curve shows it to be essentially the same as the one found when no Pd anions are incorporated into the PVP film. In other words, no appreciable amount of reduced mediator is generated by the $PdCl_4^{2-}$ in the film. This is also confirmed by the fact that the UME had to be held for a longer time close to the surface to form any noticeable pattern. Surprisingly, the patterns that are formed with the Pd-complex are ring shaped (Fig. 3c). Elemental analysis (by EDS) of the pattern showed higher concentrations of metallic palladium only on the ring, while the amount of palladium measured inside the ring was not higher than the background. Thus, $PdCl_4^{2-}$, which penetrates the PVP film upon soaking in a $PdCl_2$/HCl solution, was reduced by $Ru(NH_3)_6^{2+}$ to form Pd metal in an overall reaction

$$2Ru(NH_3)_6^{2+} + PdCl_4^{2-} \rightarrow 2Ru(NH_3)_6^{3+} + Pd + 4Cl^- \quad [3]$$

Pattern-affecting parameters.—Since the size and shape of the patterns formed determine the usefulness of this technique in microfabrication, we investigated the different parameters that affect the pattern structure. Four extrinsic factors control the size of the pattern; namely, the distance of the UME from the surface, the ratio of the radii of the insulating sheath and the microelectrode, the diameter of the microelectrode, and the electrolysis time. In other words, in a fast electron transfer process, where the reduced mediator reacts rapidly with the species in the polymer film, these factors will determine the size of the pattern produced.

UME-surface distance.—The dependence of the diameter of the pattern formed on the distance is linear, as shown in Fig. 4. A conical concentration profile is expected between the UME and the surface. This profile can be interpreted in terms of the shape of the UME and the diffusion field; *i.e.*, the relatively large insulator around the electrode provides a cylindrical volume between the UME and the surface. Inside this cylindrical volume a conical concentration profile of the reduced mediator is established by diffusion. The truncated cone volume is expected to reach a steady state in which the flux of the oxidized mediator towards the UME is equal to the flux of the reduced mediator from it. This steady state is confirmed by the fact that the current is very stable, even when the UME is maintained very close to the surface. Note that the diameter of the bigger base of the truncated cone (which is on the surface) is proportional to the distance between the surface and the UME, and thus a linear dependence between the pattern diameter and the distance is anticipated.

Insulator-electrode radii ratio.—According to simulations (5) and the qualitative picture given above, the system reaches a steady state in which the concentration of $Ru(NH_3)_6^{2+}$ is almost uniform within the cone volume, while a sharp decrease in its concentration is expected outside this cone. Therefore, a smaller insulating sheath will cause a larger diffusion range of the reduced mediator. The insulator limits the spherical diffusion of the electroactive species and consequently leads to the formation of smaller patterns. The exact dependence of the size of the patterns made, as a function of the insulator/electrode ratio is difficult to obtain because of limitations in fabrication of electrodes with smaller, yet accurately known, insulator/electrode ratios. Nevertheless, Fig. 4a shows that this behavior was obtained, *i.e.*, reducing the ratio of insulator-to-electrode radius led to the formation of bigger gold disks.

Electrode diameter.—The electrode diameter determines the steady-state current (Eq. [1]). Experiments performed with different electrodes, ranging from 10-50 μm diam, result in gold disks that are proportional to the electrode diameter (Fig. 4b). Thus, bigger gold disks are obtained when a bigger electrode is applied for the same time and at the same electrode-surface distance. Note that all of these experiments were conducted with high insulator/electrode ratios and at a constant UME-distance. Since electrodes down to 0.6 μm diameter have been fabricated, much smaller patterns can, in principle, be produced.

Electrolysis time.—Since the reduced mediator is generated at the UME and diffuses to the surface, it is expected that the electrolysis time, *i.e.*, the time during which a po-

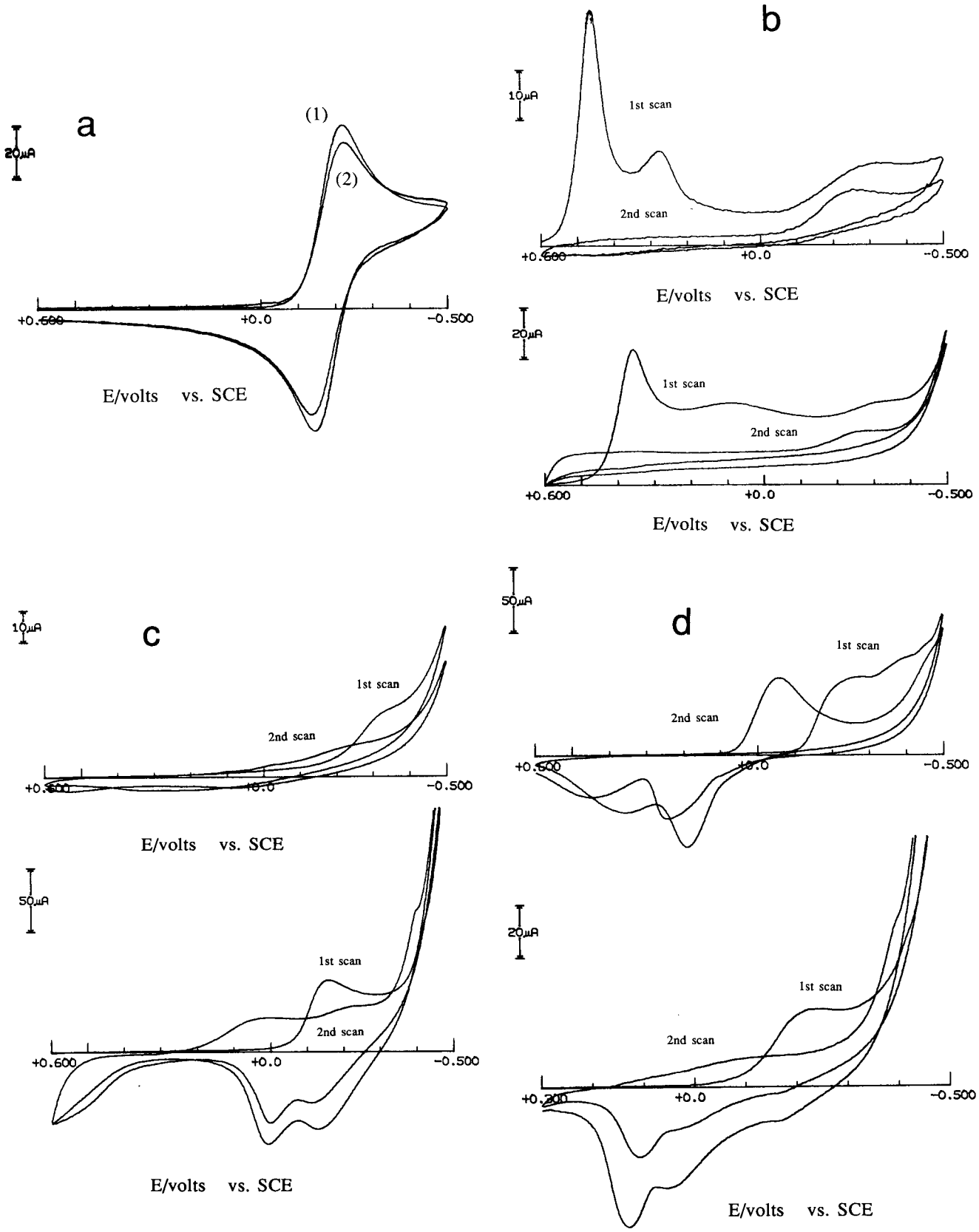

Fig. 7. Cyclic voltammograms taken with a glassy carbon electrode (GCE, 3.0 mm diam) and a scan rate of 100 mV/s. (a) In 10 mM $Ru(NH_3)_6^{3+}$/0.1M HCl solution; (1) bare electrode; (2) 1 min after immersing a PVP-coated electrode. (b) In 1 mM $NaAuCl_4$/1.0M HCl solution with a bare electrode (bottom) and in a 0.1M HCl solution with a PVP-coated electrode that was soaked in 0.05M $NaAuCl_4$/0.1M HCl solution for 30 min (top). (c) In 1 mM $PdCl_2$/0.1M HCl solution with a bare electrode (bottom) and in a 0.1M HCl solution with a PVP-coated electrode that was soaked in 0.05M $PdCl_2$/0.1M HCl for 30 min (top). (d) In 1 mM $Pd(NO_3)_2$/0.1M HBr solution with a bare electrode (bottom) and in a 0.1M HCl solution with a PVP-coated electrode that was soaked in 0.05M $Pd(NO_3)_2$/0.1M HBr solution for 30 min (top).

tential is applied to the UME, will determine the diffusion range and thus affect the size of the pattern formed. However, such behavior should be anticipated only when a fast electron transfer occurs between the mediator and the species at the film surface. Figure 5a shows the dependence of the pattern radii on the electrolysis time. The gold disks

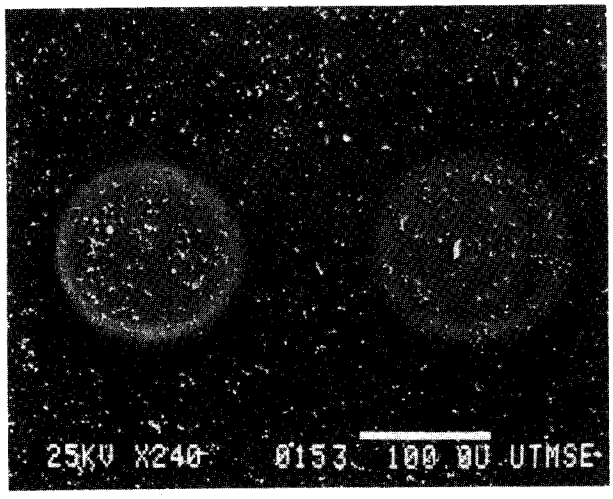

Fig. 8. Scanning electron micrograph of palladium patterns formed upon leaving a 25 μm Pt UME (E = −0.3V vs. SCE, 10 min) close to a PVP-coated substrate which was soaked in 0.05M $Pd(NO_3)_2$/0.1M HBr solution for 30 min.

grew constantly as a function of time until they reached a certain radius, and then the increase slowed, but did not stop. The sudden change in the rate of the disk formation follows the UME radii, namely, disks are rapidly formed until they match the size of the insulator of the UME. This is again interpreted in terms of the concentration profiles. Once the volume between the UME and the surface is filled with the reduced mediator, the changes in the concentration profiles will be smaller, because of the large spherical volume the mediator can diffuse into. The radii of the patterns formed within the UME limits depend on the square root of time (Fig. 5b), as is expected for a diffusion-controlled process. The diffusion distance, δ, is given by Eq. [4], where D is the diffusion coefficient and t corresponds to the electrolysis time

$$\delta \cong \sqrt{\pi D t} \qquad [4]$$

However, for the radii of the patterns to depend on the square root of time, the electrode-surface distance must be much smaller than the diffusion distance. This condition was maintained in all our experiments. The diffusion coefficient calculated from Fig. 5 is $D = 2.8 \times 10^{-8}$ cm^2 s^{-1} and is smaller than the value for $Ru(NH_3)_6^{2+}$ in homogeneous solution, since the mediator must penetrate into the polymer to reduce the metal complex. Therefore, the experimental value is a function of the diffusion coefficient in homogeneous solution and in the polymeric matrix.

The nature of the metal complex.—The main difference between the gold and the palladium samples is the shape of the patterns that are formed. The experiments are highly reproducible, and yet only gold disks are formed when the PVP-coated substrate is soaked in a $NaAuCl_4$/HCl solution, while palladium rings are observed using a $PdCl_2$/HCl solution. Varying the extrinsic parameters discussed above, such as increasing the electrode-surface distance or the electrolysis time, never resulted in a change in form, *i.e.*, palladium disks or gold rings. To account for this difference, other techniques were applied to obtain additional information about the reactions.

The electronic absorbance spectra of PVP films soaked in $NaAuCl_4$/HCl and $PdCl_2$/HCl solutions (Fig. 6A) indicate that the concentration of the gold complex in the film is higher than that of the palladium chloride anion. If we assume a similar extinction coefficient for the anions in the films and in a homogeneous solution, the concentration of gold anions is two to four times higher than that of the palladium anions.

Cyclic voltammetry supports these findings (Fig. 7b, c). A prominent reduction wave (i_{pc} = 39.2 μA) is observed during the first cycle of a glassy carbon electrode (GCE) spin coated with PVP and soaked in $NaAuCl_4$/HCl solution, while only a small reduction peak (i_{pc} = *ca.* 15 μA) is detected when the GCE is soaked in $PdCl_2$/HCl solution. In both cases, the reduction waves show no anodic waves on reversal and disappear during the second and subsequent scans. This behavior is consistent with the proposed reaction path, where the metal ions are reduced to the free metals on the cathodic potential sweep and are essentially depleted from the film during a single sweep at 100 mV/s. The anodic peaks seen at the GCE soaked in $PdCl_2$/HCl solution are probably related to the desorption of hydrogen from the electrodeposited palladium. The CV results suggest that the different shapes of the patterns might be due to the difference in the concentrations of the two species, *i.e.*, $AuCl_4^-$ and $PdCl_4^{2-}$. However, gold disks and palladium rings are still formed when either the concentration of the gold anion in the soaking solution is decreased by a factor of 100 or the palladium anion concentration is increased ten times. Moreover, gold disks are also formed when a competitive anion such as SO_4^{2-} (0.1M) is added to the soaking solution, although these disks contain a smaller amount of gold.

We feel important factors in the production of disks *vs.* rings are the ease and rate of reduction of the metal complex in the PVP by the reduced mediator. The cyclic voltammogram of $Ru(NH_3)_6^{3+}$ at a bare and PVP-coated GCE (Fig. 7a) shows that the incorporated anions are accessible to the reduced mediator. Examination of the cyclic voltammograms of the metal anions in PVP films (Fig. 7b, c) allows one to estimate the reduction potential for both complexes. The reduction of $AuCl_4^-$ occurs at 0.46V *vs.* SCE in the PVP film, with the reduction of $PdCl_2$ at −0.32V *vs.* SCE in the film. The formal potential for reduction of $Ru(NH_3)_6^{3+}$ in 0.1M HCl is $E^{o\prime}$ = −0.18V *vs.* SCE (Fig. 7a), so that the reduction of the palladium chloride anion by the reduced mediator faces a slight energy barrier, and thus will be much slower than the rate in homogeneous solution, which is very fast. This assumption is supported by other results. Figure 6B shows the electronic spectra obtained after applying −0.35V *vs.* SCE to the PVP/ITO films which were soaked in either a Pd(II) or Au(III) anionic complex solution for 30 min. The gold absorbance disappeared completely, while only small changes were detected in the film containing palladium.

To confirm this assumption relating ease and rate of reduction with deposit shape, we examined a Pd-complex that reduces at less negative potentials, $PdBr_4^{2-}$. There are two differences between the $PdBr_4^{2-}$ and the $PdCl_4^{2-}$ cyclic voltammograms. The cathodic current of $PdBr_4^{2-}$ is 3.9 times larger than that of the chloride complex, indicating that the concentration of $PdBr_4^{2-}$ in PVP is higher, assuming the diffusion coefficients of both species are essentially the same in PVP. This is supported by the electronic spectra of PVP/ITO films, which were soaked in the bromide and chloride palladium solution (Fig. 6A). According to these measurements, the concentration of $PdBr_4^{2-}$ is 5.1M, while the concentration of $PdCl_4^{2-}$ is 0.8 ± 0.3M. The second difference concerns the redox potential. The cathodic wave of $PdBr_4^{2-}$ occurs at more positive potentials than that of $PdCl_4^{2-}$; hence, this Pd complex should be reduced more easily by $Ru(NH_3)_6^{2+}$ than is $PdCl_4^{2-}$. Indeed, using the SECM in the feedback mode with $Ru(NH_3)_6^{3+}$ as a mediator and $Pd(NO_3)_2$/HBr as a soaking solution leads to a slight positive feedback current when the UME approaches the PVP surface. This is followed by the formation of Pd disks (Fig. 8) when the UME is held in position for a short time (1-2 min).

However, careful examination of the Pd disk by SEM reveals that the periphery contains a higher Pd concentration than the inner part. Possibly, the rings formed by $PdCl_4^{2-}$ reduction contain undetectable amounts of Pd in the inner part, because of the lower concentration of $PdCl_4^{2-}$ in PVP films. The accumulation of Pd in both cases in the periphery might be due to the diffusion of Pd ions towards the ring or disk regions. Nonetheless, we assume that the difference in $PdBr_4^{2-}$ and $PdCl_4^{2-}$ behavior is caused mainly by a difference in the thermodynamic redox potential rather than by a difference in the concentration of the two species in the film. Accordingly, an almost complete disappearance of the electronic absorbance of $PdBr_4^{2-}$ is observed when a potential of −0.35V *vs.* SCE

is applied to a PVP/ITO electrode that has been soaked in $Pd(NO_3)_2$/HBr (Fig. 6B).

All the results indicate that $Ru(NH_3)_6^{2+}$ is not an efficient reductant for the $PdCl_4^{2-}$ complex when the metal anion is incorporated in a polymer. Therefore, exchanging the redox couple to a stronger reductant should also lead to formation of palladium disks, even with $PdCl_4^{2-}$. Indeed, when methyl viologen, MV^{2+}, or propyl viologen sulfonate, PVS, were used as mediators, where the redox potentials of these mediator systems are much more negative ($E = -0.45$V *vs.* NHE) than that of $Ru(NH_3)_6^{3+/2+}$, palladium disks, as well as gold disks, were formed. Both metal complexes show similar behavior with viologen mediators.

Conclusions

A new approach to the high resolution deposition of metals using the SECM is presented. The SECM is operated in the feedback mode where an electrochemically generated redox couple monitors the distance between an ultramicroelectrode and a surface. We showed that when an electroactive species is incorporated in a polymer layer on the surface, the reduced mediator can be used not only to monitor the distance, but in addition can transfer an electron to the species, *e.g.*, $AuCl_4^-$, leading to the formation of high resolution structures on the surface. In this way, gold and palladium have been deposited in a polymer film.

The different factors that affect the size and the shape of the structures deposited were examined and interpreted. These include the distance between the electrode and the surface, the ratio between radii of the insulating sheath and the metal electrode, the radius of the electrode and the electrolysis time. The roles played by the metal ion to be reduced as well as the mediator were investigated by investigating different metal complexes, mediators, and techniques. We demonstrated that various combinations of metal-complex-mediator can result in different structures, according to their thermodynamic and kinetic properties. We conclude that a fast electron transfer between the generated mediator and the electroactive species at the surface is crucial in achieving any type of high resolution electrode modification, such as metal deposition.

Further applications using this approach, such as high resolution electrode modification through metal oxide formation and high resolution metal etching, are now being examined.

Acknowledgments

Dr. O. E. Hüsser is warmly acknowledged for helpful advice and discussions as well as for his assistance in SEM measurements. We also thank Mr. J. Cooke, for preparing the sputtered samples. The Chaim Weizmann Fellowship Foundation is gratefully acknowledged for supporting D. Mandler. The support of this research by the Texas Advanced Research Program and the Robert A. Welch Foundation is gratefully acknowledged.

Manuscript submitted May 30, 1989; revised manuscript received Oct. 10, 1989.

The University of Texas at Austin assisted in meeting the publication costs of this article.

REFERENCES

1. (a) D. J. Elliott, "Microlithography: Process Technology for IC Fabrication," McGraw-Hill, New York (1986); (b) W. C. Till and J. T. Luxon, "Integrated Circuits: Materials, Devices and Fabrication," Prentice-Hall, Inc., Englewood Cliffs, NJ (1982); (c) R. A. Colclaser, "Microelectronics: Processing and Device Design," 2nd ed., John Wiley & Sons, Inc., New York (1980); (d) S. M. Sze, "VLSI Technology," McGraw-Hill, Inc., New York (1988).
2. Some examples are (a) M. Hatzakis, *IBM J. Res. Dev.*, **32,** 441 (1988); (b) C. P. Umbach, A. N. Broers, R. H. Koch, C. G. Willson, and R. B. Laibowitz, *ibid.*, **32,** 454 (1988); (c) T. H. P. Chang, D. P. Kern, E. Kratschmer, K. Y. Lee, H. E. Luhn, M. A. McCord, S. A. Rishton, and Y. Vladimirsky, *ibid.*, **32,** 462 (1988); (d) C. Lyons and W. Moreau, *This Journal*, **135,** 193 (1988); (e) S. W. Pang, W. D. Goodhue, and M. W. Geis, *ibid.*, **135,** 1526 (1988); (f) C. H. Ting and M. Paunovic, *ibid.*, **136,** 456 (1989); (g) D. P. Kern, T. F. Kuech, M. M. Oprysko, A. Wagner, and D. E. Eastman, *Science*, **241,** 939 (1988).
3. (a) D. W. Abraham, H. J. Mamin, E. Ganz, and J. Clarke, *IBM J. Res. Dev.*, **30,** 492 (1986); (b) R. M. Silver, E. E. Ehrichs, and A. L. deLozanne, *Appl. Phys. Lett.*, **51,** 247 (1987); (c) M. A. McCord and R. F. W. Pease, *ibid.*, **50,** 569 (1987); (d) C. W. Lin, F.-R. F. Fan, and A. J. Bard, *This Journal*, **134,** 1038 (1987); (e) H. C. Pfeiffer, *Opt. Eng.*, **26,** 325 (1987).
4. A. J. Bard, F.-R. F. Fan, J. Kwak, and O. Lev, *Anal. Chem.*, **61,** 132 (1989).
5. (a) J. Kwak and A. J. Bard, *ibid.*, **61,** 1221 (1989); (b) J. Kwak and A. J. Bard, *ibid.*, **61,** 1794 (1989).
6. (a) D. H. Craston, C. W. Lin, and A. J. Bard, *This Journal*, **135,** 785 (1988); (b) O. H. Hüsser, D. H. Craston, and A. J. Bard, *J. Vac. Sci. Technol.*, **B6,** 1873 (1988); (c) O. H. Hüsser, D. H. Craston, and A. J. Bard, *This Journal*, **36,** 3222 (1989).
7. R. Wohlgemuth, J. W. Otvos, and M. Calvin, *Proc. Natl. Acad. Sci., U.S.A.*, **79,** 5111 (1982).
8. (a) R. M. Wightman and D. O. Wipf, *J. Electroanal. Chem.*, **15,** 267 (1989); (b) M. Fleishmann, S. Pons, D. Rolison, and P. P. Schmidt, "Ultramicroelectrodes," Datatech Systems, Morganton, NC (1987).
9. (a) N. Oyama and F. C. Anson, *This Journal*, **127,** 247 (1980); (b) N. Oyama and F. C. Anson, *Anal. Chem.*, **52,** 1192 (1980); (c) N. Oyama, K. Sato, and H. Matsuda, *J. Electroanal. Chem.*, **115,** 149 (1980).
10. F. M. Lever and A. R. Powell, *J. Chem. Soc.*, A1477 (1969).

Reprinted from JOURNAL OF THE ELECTROCHEMICAL SOCIETY
Vol. 137, No. 4, April 1990
Printed in U.S.A.